Kinetics of the Reactions of Vinyl (C_2H_3) and Propargyl (C_3H_3) Radicals with NO_2 in the Temperature Range 220−340 K

Wolf D. Geppert,‡ Arkke J. Eskola, Raimo S. Timonen,* and Lauri Halonen

Laboratory of Physical Chemistry, P.O. Box 55 (A.I. Virtasen aukio 1), FIN-00014 University of Helsinki, Helsinki, Finland

Received: October 7, 2003; In Final Form: March 4, 2004

The kinetics of the reactions of vinyl (C_2H_3) and propargyl (C_3H_3) radicals with NO_2 have been studied in direct measurements at temperatures between 220 and 340 K, using a tubular flow reactor coupled to a photoionization mass spectrometer. The vinyl and propargyl radicals have been homogeneously generated at 193 nm by the pulsed laser photolysis of methyl vinyl ketone (vinyl bromide) and propargyl chloride, respectively. Decays of radical concentrations have been monitored in time-resolved measurements to obtain the reaction rate coefficients under pseudo-first-order conditions with the amount of NO_2 being in large excess over radical concentrations. The bimolecular rate coefficients of both reactions are independent of the bath gas (He or N_2) and pressure within the experimental range (1−7 Torr) and are found to depend on temperature as follows: $k(C_2H_3 + NO_2) = [(4.19 \pm 0.05) \times 10^{-11}](T/300\ \mathrm{K})^{-0.60 \pm 0.07}$ cm^3 molecule^{-1} s^{-1} and $k(C_3H_3 + NO_2) = [(2.55 \pm 0.05) \times 10^{-11}](T/300\ \mathrm{K})^{-1.06 \pm 0.10}$ cm^3 molecule^{-1} s^{-1}, with the uncertainties given as 1 standard deviation. The photolysis of propargyl chloride has also been observed to produce $C_3H_3Cl_2$ radicals rapidly under the experimental conditions, thus enabling us to measure the bimolecular reaction rate coefficient of the $C_3H_3Cl_2$ radical with NO_2 at room temperature: $k(C_3H_3Cl_2 + NO_2) = (2.37 \pm 0.05) \times 10^{-11}$ cm^3 molecule^{-1} s^{-1}. Estimated overall uncertainties in the measured bimolecular reaction rate coefficients are about ±20%. The only reaction product observed for the vinyl radical reaction with NO_2 is NO. The experimental findings have been compared with the results of ab initio calculations, which give insight into possible reaction pathways.

Introduction

Unsaturated hydrocarbon species such as vinyl (C_2H_3) and propargyl (C_3H_3) radicals are regarded as important intermediates in hydrocarbon combustion processes. This is due to their important role in the formation of polycyclic aromatic hydrocarbon (PAH) molecules and in the buildup of soot.[1,2] In this respect, the vinyl radical, the simplest alkenyl radical, is a particularly significant species in acetylene-rich enviroments.[2,3] For example, benzene can be formed in a reaction sequence consisting of an H-atom addition to C_2H_2 (forming the vinyl radical) followed by successive C_2H_2 addition and back-formation of H, making a catalytic cycle.[2,3] However, under oxygen-rich conditions, the vinyl radical concentration is suppressed by a rapid reaction between the vinyl radical and molecular oxygen.[4,5] On the other hand, the propargyl radical possesses notable resonance stabilization and is an exceptionally stable hydrocarbon free radical, which, consequently, reacts only slowly with molecular oxygen.[6,7] At room temperature, the vinyl radical reacts about 40 time faster with molecular oxygen than the propargyl radical.[4−7] Thus, the propargyl radical may attain relatively high concentration in flames. The fast recombination of propargyl radicals followed by a ring closure and rearrangement is believed to be an important formation pathway of benzene in fuel-rich flames.[1,8,9]

Since NO and NO_2 are produced in considerable amounts in hydrocarbon combustion, it is worth investigating the extent to which NO_2 can retard the formation of PAH compounds and soot by reacting with their precursors, i.e. vinyl and propargyl radicals. However, in contrast to the abundance of research on other reactions of hydrocarbon radicals, kinetic data on reactions of unsaturated hydrocarbon radicals with NO_2 are sparse.[10] Slagle et al.[11] have measured the room temperature rates of the reaction of the allyl (C_3H_5) radical with NO_2 and identified NO and C_3H_5O as the only primary products. No data exist for the reactions of unsaturated hydrocarbon free radicals with NO_2 at temperatures lower than 298 K.

In addition to the experimental interest, the R + NO_2 (R = the vinyl or propargyl radical) reactions are also worth computational investigation. It is rewarding to compare reaction mechanisms of a relatively stable radical (propargyl) with a reactive one (vinyl). The hydrocarbon radical can attack on the nitrogen atom of the NO_2 molecule, which leads to a nitro (RNO_2) intermediate, or on one of the oxygen atoms forming nitrite (RONO), both of which can form different end products. In addition to the attack of NO_2 to the CH_2 site of the propargyl radical, the approach of NO_2 at the acetylenic end of the propargyl radical leading to allenyl nitrite ($H_2CCCHONO$) or nitroallene ($H_2CCCHNO_2$) cannot entirely be ruled out. Since the propargyl radical can be described as a resonance structure with almost equal contribution from the allenyl and propargyl forms,[12] pathways with allenyl intermediates can contribute substantially to the total reaction. All intermediates can lead to different final products. A further possible pathway is the direct

* To whom correspondence should be addressed. E-mail: raimo.timonen@helsinki.fi.

‡ Current address: Department of Molecular Physics, Alba Nova, University of Stockholm, Roslagstullbacken 21, S-10691 Stockholm, Sweden.

10.1021/jp0370167 CCC: $27.50
Published on Web 04/15/2004

abstraction of an H atom by NO_2 to form HNO_2 (e.g., R + $NO_2 \rightarrow R_{-H} + HNO_2$), which in the presence of NO_2 is assumed to take place in the formation of olefins during the photooxidation of isobutene.[13] Our treatment is based on a two-body mechanism, but the possibility of three-body addition reactions (R + [M] + $NO_2 \rightarrow RNO_2/RONO$ + [M]) also has to be investigated. An analogous mechanism has been identified to occur in the $C_3H_3 + O_2$ reaction at low temperatures.[14]

This paper presents kinetic measurements of the $C_2H_3 + NO_2$ and $C_3H_3 + NO_2$ reactions in the atmospheric temperature range between 220 and 336 K. Ab initio calculations of the energies of reactants, intermediates, and products are used to illustrate reaction pathways and to explain the formation of the observed NO product.

Experimental Section

Details of the experimental apparatus and procedures used have been described previously,[5] so only a brief overview is given here. The gas mixture flowing through a tubular reactor contained the radical precursor (<0.05%), NO_2 in varying amounts, and an inert carrier gas (He or N_2) in large excess (>99.8%). Vinyl and propargyl radicals were homogeneously generated from an appropriate precursor at 193 nm by pulsed unfocused excimer laser (ELI-76E) photolysis along the flow reactor. Gas flow through the tubular, temperature-controlled reactor was about 5 m s^{-1}, which ensured that the gas mixture was completely replaced between laser pulses with the repetition rate of 5 Hz. The two reactor tubes with 6 and 17 mm inner diameters (i.d.) employed were made of seamless stainless steel and were coated with halocarbon wax.[5]

The gas mixture was continuously sampled through a 0.4 mm diameter hole at the side of the reactor and formed into a beam by a conical skimmer before it entered a vacuum chamber containing a photoionization mass spectrometer (PIMS). As the gas beam traversed the ion source, a portion was photoionized and the ions formed were mass selected in the quadrupole mass spectrometer (Extrel, C-50/150-QC/19 mm rods). Ionization radiation in the PIMS was provided by atomic resonance lamps: a Cl-lamp (8.9−9.1 eV) for C_3H_3 and $C_3H_3Cl_2$, a H-lamp (10.2 eV) for C_2H_3, CH_3, $CH_3C(O)CH_3$, methyl vinyl ketone (MVK), C_3H_3Cl (chloroallene), NO, and NO_2, and an Ar-lamp (11.6−11.8 eV) for C_3H_3Cl (propargyl chloride). Temporal ion signal profiles were recorded by a multichannel scaler (EG&G Ortec MCS plus) from 10 ms before each laser pulse up to 80 ms following the pulse. Typically, a signal profile from 3000 to 15000 repetitions was accumulated before the data were fitted by the least-squares method to an exponential function, $[R]_t = [R]_0 \exp(-k't)$, where $[R]_t$ is the radical concentration at time t and k' is the first-order rate coefficient.

The vinyl radicals were generated from MVK[15]

$$CH_3C(O)C_2H_3 + h\nu\ (193\ nm) \rightarrow C_2H_3 + CH_3 + CO \quad (1)$$

or from vinyl bromide[16]

$$C_2H_3Br + h\nu\ (193\ nm) \rightarrow C_2H_3 + Br \quad (2a)$$

$$\rightarrow C_2H_2 + HBr \quad (2b)$$

Vinyl bromide was used as a precursor to avoid contributions from the CH_3 radicals ($CH_3 + NO_2 \rightarrow CH_3O + NO$) when the formation of the NO product was measured. Propargyl radicals were produced from propargyl chloride[6,17]

$$HCCCH_2Cl + h\nu\ (193\ nm) \rightarrow HCCCH_2 + Cl \quad (3)$$

Two other products of propargyl chloride photolysis at 193 nm (no NO_2 present) were observed at the mass versus charge ratio m/z 74 (H-lamp) and 109 (Cl-lamp). Recently, Atkinson and Hudgens[18] have studied the kinetics of the Cl-atom addition reaction to propargyl chloride at 298 K and about 5 Torr pressure giving a bimolecular reaction rate coefficient $k(Cl + C_3H_3Cl) = (1.2 \pm 0.2) \times 10^{-10}$ cm^3 $molecule^{-1}$ s^{-1}. Combining an end-product analysis with ab initio calculations, these authors together with Hudgens and Gonzalez[19] have concluded that the formed adduct possesses enough energy to rearrange to chloroallene ($H_2CCCHCl$) and a Cl-atom or to a 1,2-dichloroallyl radical ($H_2CC(Cl)CHCl$), which is the only persistent radical. This is consistent with our findings. At m/z 74, a characteristic signal for product formation was observed with use of an H-lamp. The signal reached a constant value within about 4 ms after the photolysis and it was assigned to chloroallene (IE (ionization energy) = 9.57 eV).[20] Note that because IE = 10.8 eV for propargyl chloride[20] is higher than the H-lamp energy (10.2 eV), the product signal at m/z 74 cannot originate from propargyl chloride. Similarly, using a Cl-lamp, the signal at m/z 109 reached a maximum value within about 4 ms (signal rise time less than 1 ms), after which a slow first-order decay (rate ~10 s^{-1}) was observed. This signal was assigned to the 1,2-dichloroallyl radical (IE ≈ 8.2 eV).[18]

For the reaction of the vinyl radical with NO_2, the only detected product was NO. Other potential products that were searched for but not detected for this reaction include CH_3CO, $C_2H_3NO_2$, C_2H_2, HNO_2, and C_2H_3O. In the reaction mixture containing both propargyl and 1,2-dichloroallyl radicals and NO_2 as reactant, the only detected product was also NO. Other potential products that were searched for but not detected include C_3H_2, $C_3H_3NO_2$, C_3H_3O, HNO_2, $C_3H_3Cl_2O$, $C_3H_3Cl_2NO_2$, and $C_3H_3Cl_2ONO_2$. In fact, a small signal at m/z 38 (H-lamp), characteristic for the C_3H_2 radical, was observed after the photolysis of the propargyl chloride when no NO_2 was present. This signal decayed rapidly to the baseline as NO_2 was added and no sign of the product formation was observed at m/z 38.

Radical precursors, MVK (Aldrich, purity >99%), C_2H_3Br (Aldrich, purity 98%), C_3H_3Cl (Aldrich, purity 98%), and NO_2 (Merck, purity 98%) were degassed before use. Helium (Messer-Griesheim purity of 99.9996%) and nitrogen (Aga purity of 99.9999%) were employed as supplied. The NO_2 gas was diluted in He to form a 5% mixture and was stored in a blackened glass bulb.

Computational Details

The GAUSSIAN 98 program package was used for ab initio calculations.[21] All geometries on the potential energy surfaces were optimized without symmetry constraints. For all singlet species and surfaces spin restricted methods (second-order Møller−Plesset perturbation theory, RMP2) were used, otherwise unrestricted methods have been employed. The energies obtained were corrected for zero-point contributions. Vibrational frequencies, calculated at the same level, were used for the characterization of the minima and saddle points as well as for zero-point energy corrections. For the potential surface calculations of the NO_2 attack on the vinyl and propargyl radical, structure optimizations were carried out for different fixed distances between an atom (N or O) in NO_2 and the C-atom involved in the reaction with no restriction on the symmetry or the other coordinates of the system. Calculations were performed at the MP2/6-311+G(d,p) level for the $C_2H_3 + NO_2$ reaction. Because of the higher amount of computing time required for

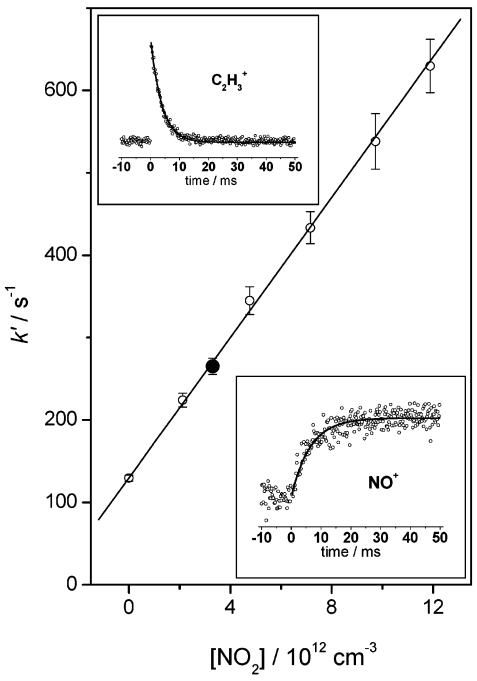

Figure 1. Plot of the first-order C_2H_3 rate coefficient k' vs $[NO_2]$ at $T = 298$ K and $P = 2$ Torr in a 6 mm i.d. reactor tube. Inserts show typical ion signal profiles for the C_2H_3 decay and the NO formation under the conditions of the solid circle in the plot: $[NO_2] = 3.3 \times 10^{12}$ molecule cm^{-3}, $k'_{decay}(C_2H_3) = 260 \pm 5$ s^{-1} ($k'_{rise}(NO) = 157 \pm 7$ s^{-1}), and $k_{wall} = 130 \pm 4$ s^{-1}. Uncertainties are 1 standard deviation (1σ).

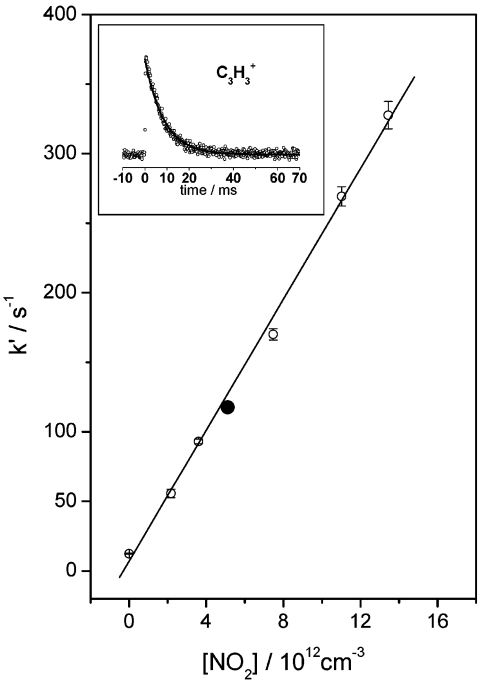

Figure 2. Plot of the first-order C_3H_3 rate coefficient k' vs $[NO_2]$ at $T = 336$ K and $P = 6$ Torr in a 6 mm i.d. reactor tube. The insert shows a typical ion signal profile for the C_3H_3 decay under the conditions of the solid circle in the plot: $[NO_2] = 5.1 \times 10^{12}$ molecule cm^{-3}, $k'_{decay} = 117 \pm 3$ s^{-1}, and $k_{wall} = 12 \pm 1$ s^{-1}. Uncertainties are 1 standard deviation (1σ).

the $C_3H_3 + NO_2$ reaction, calculations were only carried at the MP2/6-31+G(d) level for this process.

Results and Discussion

The decay of R (R = the vinyl or propargyl radical) was first monitored in time-resolved experiments without NO_2 to obtain the wall reaction rate coefficient, k_{wall}, which was measured by reducing precursor concentration and/or laser intensity (1−10 mJ cm^{-2}) until the rate obtained for this process no longer depended on these parameters and an exponential fit to the temporal ion signal showed no deviation from a first-order decay. When these conditions were achieved, it was presumed that all radical−radical processes were suppressed (i.e., that those had negligible rates compared to the first-order processes occurring in the system). Initial R concentrations were then typically below 2×10^{11} molecules cm^{-3}, which was estimated from the measured decompositions of the precursors or from the laser fluences and known absorption cross-sections and quantum yields of the precursor at 193 nm. Note that although both procedures were employed to estimate initial vinyl radical concentrations, the first method could not be used to estimate the decomposition of propargyl chloride because of the fast formation of chloroallene at the same *m*/*z* ratio. Experiments were mainly performed with relatively high precursor concentration [$\sim(5-50) \times 10^{12}$ molecules cm^{-3}] but with low laser intensity to minimize NO_2 decomposition. A few experiments were carried out with lower precursor concentration and higher laser intensity to test the possible importance of radical−precursor reactions. It was found that changes in precursor concentration had a minor or no effect on k_{wall} and no effect on $k(R + NO_2)$.

The first-order rate coefficient (k') was measured as a function of the NO_2 concentration ($[NO_2]$), which was always much higher than [R], resulting in pseudo-first-order reaction kinetics. Since the only significant processes consuming R during these experiments were the reaction with NO_2 and k_{wall}, the bimolecular reaction rate coefficient $k(R + NO_2)$ could be obtained from the slope of the k' vs $[NO_2]$ plot. These are shown in Figures 1 and 2 with typical examples of the vinyl and propargyl radical signal decays, respectively. The formation profile of the NO product signal is also shown for the $C_2H_3 + NO_2$ reaction with C_2H_3Br as the precursor. In this case, the origin of the NO signal can be assigned to the $C_2H_3 + NO_2$ reaction, because C_2H_3 was the only reactive radical formed in the photolysis (the Br atom does not react with precursor or NO_2 within the time scale of measurements, i.e., about 50 ms)[10] and a subsequent reaction of the C_2H_3O product with NO_2 should not produce NO.[22] However, the value obtained for $k'_{rise}(NO)$ differs from $k'_{decay}(C_2H_3)$ probably because of the lower detection sensitivity for NO compared to C_2H_3 and the formation of NO from NO_2 in the laser pulse at 193 nm. The formation of NO was also observed after the photolysis of the gas mixture containing both NO_2 and propargyl chloride, but the noisy signal and the presence of two different radicals (C_3H_3, $C_3H_3Cl_2$) made it impossible to assign unambiguously the origin of NO.

As mentioned, some NO_2 was photolyzed in the laser pulse at 193 nm according to the following reaction[23]

$$NO_2 + h\nu\ (193\ nm) \rightarrow NO + 0.55\ O(^1D) + 0.45\ O(^3P) \quad (4)$$

Oxygen atom concentration was suppressed by using low laser intensity and high appropriate precursor concentration. The decomposition of NO_2 at 193-nm photolysis was estimated from the absorption cross-section[23] and the laser intensity and found to lie between 0.03% and 0.3%. Experiments performed with higher laser intensity ($\sim$10 mJ cm^{-2}) and lower precursor concentration yielded essentially the same values within the experimental uncertainty for the bimolecular rate coefficients.

TABLE 1: Results and Conditions of the Experiments[a] Used To Measure the Bimolecular Rate Coefficients of the Reaction R + NO_2 → Products (R = C_2H_3, C_3H_3, and $C_3H_3Cl_2$)

T/K	P^b/Torr	10^{-12}[NO_2]/cm^{-3}	$d_{reactor}$/mm	k_{wall}/s^{-1}	$10^{11}k^c$/cm^3 s^{-1}
R = C_2H_3, (C_2H_3 + NO_2 → C_2H_3O + NO)					
$k(C_2H_3 + NO_2) = [(4.19 \pm 0.05) \times 10^{-11}](T/300\ K)^{-0.60\pm0.07}$ cm^3 s^{-1}					
220	1.0	1.6−6.3	17	40	5.23 ± 0.16
220	1.8	1.7−9.4	6	88	4.73 ± 0.10
242	1.0	1.6−7.2	17	38	4.85 ± 0.15
267	1.0	1.5−6.5	17	38	4.52 ± 0.10
298	1.0	1.2 −6.3	17	26	4.30 ± 0.08
298	4.0	1.9 −6.6	17	25	4.20 ± 0.18
298	1.0[d]	1.6−6.1	17	27	4.39 ± 0.15
298[e]	2.2	2.1−11.9	6	129	4.15 ± 0.06
298[e]	4.0	1.9−6.1	17	25	4.12 ± 0.10
336	1.0	1.5−7.6	17	26	3.87 ± 0.06
336	1.8	2.3−11.1	6	77	3.86 ± 0.06
R = C_3H_3, (C_3H_3 + NO_2 → products)					
$k(C_3H_3 + NO_2) = [(2.55 \pm 0.05) \times 10^{-11}](T/300\ K)^{-1.06\pm0.10}$ cm^3 s^{-1}					
220	6.0	2.0−8.3	6	11	3.61 ± 0.05
242	6.0	2.2−11.5	6	11	3.23 ± 0.06
242	7.1	2.7−9.8	6	9	2.98 ± 0.05
241	2.0	3.7−12.3	17	7	3.42 ± 0.09
267	5.8	2.1−9.6	6	13	2.92 ± 0.05
298	6.0	2.2−11.8	6	5	2.52 ± 0.04
298	6.0	2.3−13.1	6	9	2.63 ± 0.10
298	2.1	3.4−14.8	6	7	2.40 ± 0.05
298	2.9[d]	1.9−10.6	6	19	2.63 ± 0.04
298	2.0	4.5−11.0	17	8	2.55 ± 0.06
336	5.8	2.2−13.5	6	12	2.35 ± 0.06
R = $C_3H_3Cl_2$, ($C_3H_3Cl_2$ + NO_2 → products)					
$k_{298}(C_3H_3Cl_2 + NO_2) = (2.37 \pm 0.05) \times 10^{-11}$ cm^3 s^{-1}					
298	2.1	3.0−12.6	17	7	2.37 ± 0.06
298	6.1	2.3−10.5	17	8	2.37 ± 0.07

[a] Range of precursor concentrations used: (1.4 − 6.7) × 10^{12} molecule cm^{-3} for MVK, (4.9 − 16) × 10^{12} molecule cm^{-3} for C_2H_3Br, and (5.9 − 52) × 10^{12} molecule cm^{-3} for C_3H_3Cl. Laser intensities used were 1−10 mJ/cm^2. Estimated initial radical concentrations were 0.8−2.9 × 10^{11} molecule cm^{-3}. [b] Helium used as a buffer gas unless otherwise stated. [c] Statistical uncertainties shown are 1σ; estimated overall uncertainty is ±20%. [d] Nitrogen used as a buffer gas. [e] C_2H_3Br used as a precursor.

The equilibrium between NO_2 and N_2O_4 is shifted toward the dimer at low temperatures.[24] However, in our system, the amount of NO_2 converted to N_2O_4 was insignificant (<0.1%) because of the low NO_2 concentrations used and because of the small value of the equilibrium coefficient at room temperature. In addition, the equilibrium was not reached within the short residence time (∼100 ms) in the cooled zone of the reactor because the recombination rate for dimer formation ($k' \approx 0.013$ s^{-1}) is slow under experimental conditions.[25] Such a small amount of dimer does not have any significant effect on our results.

Investigations were also carried out to find out the possible presence of second-order R (R = the vinyl or propargyl radical) heterogeneous wall reactions. Both 17 mm and 6 mm i.d. reactor tubes with the same coatings were employed to vary the surface-to-volume ratio (almost by a factor of 3).[5,26] One would expect a higher bimolecular reaction rate coefficient k(R + NO_2) for the 6 mm than for the 17 mm i.d. tube, if second-order heterogeneous reactions occurred in any significant extent. This was not observed and only the first-order wall reaction rate coefficient k_{wall} was higher for the 6 mm than for the 17 mm i.d. tube. We concluded that second-order wall reactions are unimportant in our experiments.

The measured bimolecular reaction rate coefficients for the vinyl and propargyl radical reactions with NO_2 are shown in Table 1 with their statistical uncertainties (1σ) and experimental conditions. Estimated overall uncertainties in measured bimolecular reaction rate coefficients are about ±20%. These arise mainly from the uncertainties in determining reactant concentrations and from the uncertainties in decay rate coefficients. Linear least-squares fits to an expression $k = A \times (T/300\ K)^n$, where T is temperature in K, and A and n are empirical parameters, are given in Table 1. Corresponding results for the 1,2-dichloroallyl radical at 298 K are also given. Double-logarithmic plots of the bimolecular rate coefficients for the vinyl and propargyl radical reactions with NO_2 are shown in Figure 3.

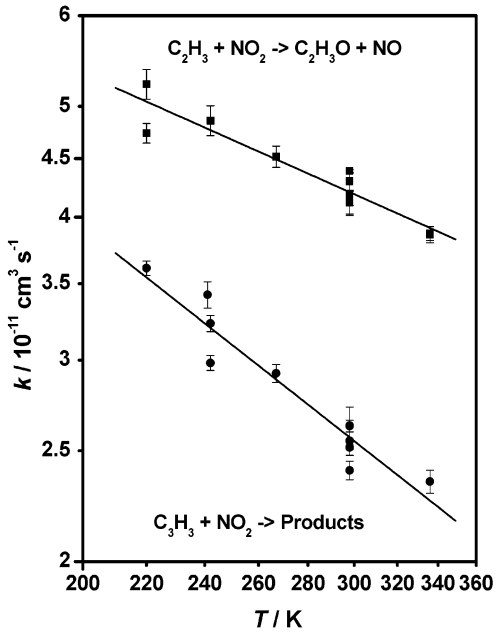

Figure 3. Double-logarithmic plots of the measured bimolecular rate coefficients versus T.

The higher rate of the C_2H_3 + NO_2 reaction compared to that of the C_3H_3 + NO_2 reaction can be explained by the reactivity of the vinyl radical. A similar difference in reaction rates has been found in the C_2H_3 + Br_2 and C_3H_3 + Br_2 reactions, where the difference in rates is even more prominent at temperatures overlapping with present experiments.[27] No evidence of an activation barrier was observed in any of the two reactions, but the existence of a very small activation barrier (<2.5 kJ mol^{-1}) cannot be excluded, since the experiments were not conducted at temperatures lower than 220 K. Nevertheless, a centrifugal barrier, which increases with rising relative translational energy of the reactants, is the only rate-determining feature at the temperatures used. Since the title systems can be regarded as radical−radical reactions, such a behavior is hardly surprising, but the high exponential temperature factors of both fits should be noted. A lower temperature dependence ($k \propto T^{-1/6}$) has been predicted by using classical capture theory and electrostatic potentials for different interactions in the case of a related reaction of two neutral $^2\Pi$ molecules.[28] This is somewhat at odds with the present findings. However, the title reactions are not the only radical processes which show strongly negative temperature dependence. The bimolecular rate coefficient of the CN + NH_3 reaction was found to be proportional to $T^{-1.14}$.[29] In the OH + OH system, the large negative temperature dependence of the reaction rate coefficient was explained by increased population of a nonreactive spin−orbit component (such an effect is impossible in the present reactions) and an increased population of higher rotationally excited states, which could possess lower capture cross sections.[30] Rotational excita-

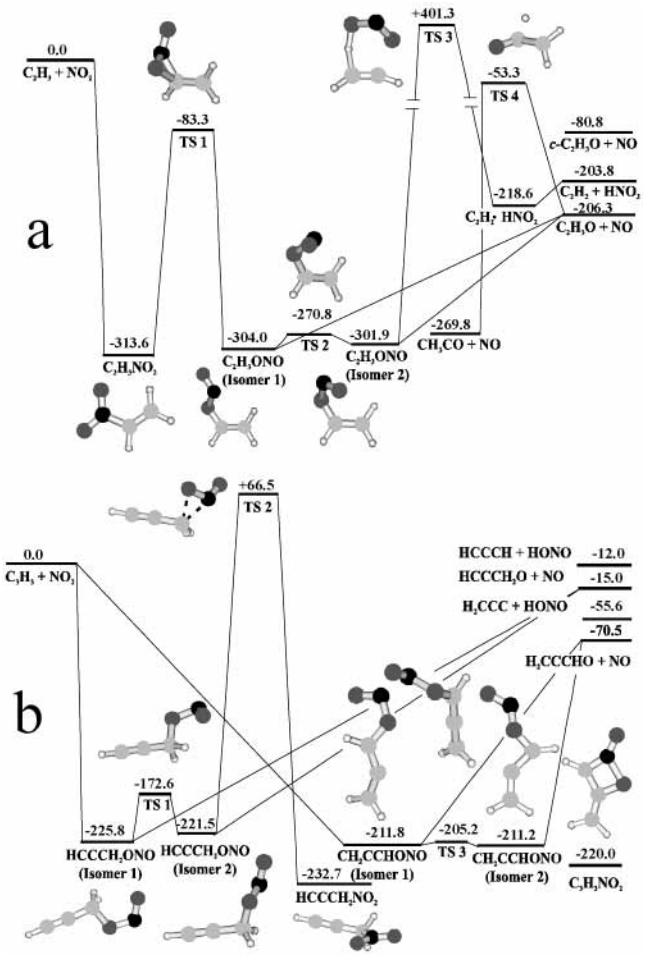

Figure 4. Energetics of the $C_2H_3 + NO_2$ reaction (a) calculated at the RMP2/6-311+G(d,p) level and the $C_3H_3 + NO_2$ reaction (b) calculated at the RMP2/6-31+G(d) level. Energies are relative to the reactants and are given in kJ/mol.

tion may cause this reduction preventing the reaction partners to find the most favorable orientation for the reaction.[31]

Measurements were carried out at different pressures to investigate possible contributions of three-body processes. Changes of the pressure between 1 and 4 Torr did not alter the rates in the $C_2H_3 + NO_2$ reaction. Therefore, no fast three-body processes are present in this system. Because of the small molecular sizes, it is also unlikely that the reaction proceeds at the high-pressure limit already at these experimental conditions. Changes of the pressure between 2 and 6 Torr did not alter rates in the analogous propargyl radical reaction. Therefore, also in this case, three-body processes do not play any important role. These findings are different from the ones obtained for the $C_3H_3 + O_2$ and $C_3H_3 + NO$ reactions, where strong pressure dependencies of the rate coefficients were observed under similar experimental conditions.[6,32]

Confining the reactions to two-body systems, several pathways for the vinyl and propargyl radical reaction with NO_2 are exoergic. The following information on possible pathways is from our ab initio calculations, see Figure 4 and the text later:

$$C_2H_3 + NO_2 \rightarrow C_2H_3O \text{ (non-cyclic)} + NO \quad (5a)$$

$$\rightarrow C_2H_3O \text{ (cyclic)} + NO \quad (5b)$$

$$\rightarrow CH_3CO + NO \quad (5c)$$

$$\rightarrow C_2H_2 + HNO_2 \quad (5d)$$

$$C_3H_3 + NO_2 \rightarrow HCCCH_2O + NO \quad (6a)$$

$$\rightarrow H_2CCCHO + NO \quad (6b)$$

The products of the reactions 5a and 5c can be formed by exoergic rearrangement of the initially produced non-cyclic vinyloxy (CH_2CHO) radical. The propargyloxy product (reaction 6a) is produced from an attack of NO_2 on the 1-C atom, whereas the formation of the allenyloxy (reaction 6b) radical is caused by a NO_2 attack on the 3-C atom. As in the analogous $C_2H_3 + NO_2$ reaction, rearrangement of the C_3H_3O products to more stable cyclic or non-cyclic isomers cannot be excluded. Several non-cyclic low-energy isomers of C_3H_3O, which can interconvert, have already been identified.[33]

Energies of the products and intermediates of the $C_2H_3 + NO_2$ reaction were calculated at the RMP2/6-311+G(d,p) level and are presented in Figure 4a. It is seen that the three major intermediate products [nitroethylene ($C_2H_3NO_2$) and two vinyl nitrite isomers (C_2H_3ONO)] are connected by transition states with barriers below the reactant energies. Although, according to the calculations, a coplanar N-site attack of NO_2 is favored, the excited nitroethylene formed can surmount the barrier to vinyl nitrite and subsequently decompose into the vinyloxy radical and to the detected NO molecule. To assess the possibility of an intermediate formation of vinylnitrite, geometry optimizations were also carried out starting from geometries resembling an O-attack on the C_2H_3 moiety at different fixed C−O distances and all other geometry parameters variable. In these cases, NO_2 rearranged itself to the geometry resembling the N-attack. Similar nitrite−nitro rearrangements were also predicted by ab initio calculations in other systems.[34−36] Wodtke et al.[37] detected experimentally the formation of CH_3O in the unimolecular decomposition of nitromethane, which gives direct evidence for nitrite−nitro rearrangements. The vinyloxy radical produced in this reaction can further isomerize via a transition state lower in energy than that of the reactants.

The potential surface obtained for the $C_2H_3 + NO_2$ system is similar to the one published previously by Gindulyté et al.[38] except that a low-lying transition state for the HNO_2 elimination was not found in our calculations. These authors predicted a relatively low barrier for the thermodynamically advantageous elimination of HNO_2 in the $C_2H_3 + NO_2$ reaction. This prediction seems to disagree with our experimental observations. We found a transition state leading to a $C_2H_2 \cdot HNO_2$ van der Waals cluster, although it is too high in energy to be surmounted under the present experimental conditions. This transition state was identified as the one leading to the HNO_2 and C_2H_2 products. It also contained an oscillation of an H-atom between carbon and oxygen as the only mode with an imaginary frequency. The lowest transition state for HNO_2 elimination depicted in ref 38 might be connecting nitroethylene with an oxohydroxylamine derivate ($H_2CCN(O)OH$, denoted as structure **3** in ref 38). In this context, it should be mentioned that the HNO_2 elimination has been observed in the decomposition of nitroalkanes.[37]

The existence of the entrance barrier of the reaction is an important issue. Both title reactions can be regarded as recombination processes between two radicals for which one would hardly expect substantial activation energy. Potential energy surfaces for the singlet (at the RMP2/6-311+G(d,p) level) and triplet (at the UMP2/6-311+G(d,p) level) states were calculated by fixing the C−N distance and optimizing all other geometrical parameters for the $C_2H_3 + NO_2$ reaction. These calculations yielded a barrier of 44.6 kJ/mol at a large C−N distance (3.4 Å). This is at odds with the experiments, since

such a result would yield a different dependence of the reaction rate on temperature. Taking into account the level of the computational method, it cannot be excluded that the barrier is an artifact of the calculation. However, a further complication arises because there exists a low-lying triplet $C_2H_3NO_2$ surface, which also shows a barrier (which is probably an avoided crossing between two triplet states), but at much shorter C−N distances (1.8 Å) than the singlet surface. At 2.8 Å, the geometries of the triplet and singlet states are similar and the energies of both states are less than 5 kJ/mol above the reactant energies. Therefore, there is a possibility that the system may approach on the triplet surface and then undergo intersystem crossing at the intersection distance to the singlet surface, thus completing the reaction without having to transgress a nonnegligible activation barrier.

A potential energy surface of the $C_3H_3 + NO_2$ reaction calculated with the RMP2/6-31+G(d) ab initio method was obtained and is presented in Figure 4b. Calculations were only carried at this level because of the expense of computing time. A barrierless pathway leading to both allenyl nitrite (H_2-CCCHONO) and propargyl nitrite ($HCCCH_2ONO$) has been found in contrast to the vinyl + NO_2 reaction. Both nitrites possess two rotameres, which are connected by low-lying transition states. The intermediate nitrites can easily undergo an NO elimination to form allenyloxy (H_2CCCHO) or propargyloxy radicals ($HCCCH_2O$), respectively. It was impossible to draw conclusions about the preferred product since (probably because of the difficulties in detecting oxy radicals with the method used) we were unable to see any C_3H_3O radicals. Regarding the final products, the $H_2CCCHO + NO$ pathway is thermodynamically favored, but given the high rates of the reaction and the absence of barriers, our results provide little insight into the pathway followed by the nitrite formation. It should be noted that, in contrast to the $C_2H_3 + NO_2$ reaction, there exists a barrier for nitrite−nitro isomerization that exceeds the reactant energies. Therefore, the formation of nitropropyne ($HCCCH_2NO_2$) does not seem to play an important role in this system. It should also be mentioned that no energy minimum was found for the nitroallene ($H_2CCCHNO_2$) structure, although its existence has been claimed by an earlier theoretical study carried out at the Hartree−Fock level.[39] Instead, a minimum resembling a structure of a four-membered oxazetidine derivative (4-methylene-2-oxo-1,2-oxazetidine shown in Figure 4b) was observed. In this context, it is interesting to note that, although the chemistry of nitroalkenes is well-documented, the information about nitroallene is sparse. There is an isolated claim of its synthesis,[40] but the paucity of reported work on such a simple organic compound suggests that it might be unstable. Therefore, the reaction pathway over nitroallene was disregarded. Finally, the possibility of a direct abstraction of hydrogen leading to HNO_2 and H_2CCC or HCCCH should be considered. The former process is exoergic whereas the latter one is almost thermoneutral. No transition states were located for these reaction channels, which supports the observation that HNO_2 was not detected in our experiments. Moreover, a transition state could not be located for the analogous C_2H_3-$NO_2 \rightarrow HNO_2 + H_2CC$ elimination.[38] In the case of the almost thermoneutral channel leading to HNO_2 and HCCCH, the existence of a barrierless process is unlikely given the considerable barrier found for the HNO_2 elimination of C_2H_3ONO.

A comparison on the reactivity of unsaturated hydrocarbon radicals (vinyl, allyl, and propargyl) with NO_2 at room temperature can now be made. Both allyl and propargyl radicals possess notable resonance stabilization while vinyl does not. The bimolecular rate coefficient obtained in this study for the vinyl radical reaction with NO_2 at 300 K, $(4.19 \pm 0.05) \times 10^{-11}$ cm^3 $molecule^{-1}$ s^{-1}, is the same within the experimental uncertaintity as the bimolecular rate coefficient obtained by Slagle et al., $(3.9 \pm 0.8) \times 10^{-11}$ cm^3 $molecule^{-1}$ s^{-1}, for the allyl radical reaction with NO_2. Our present rate coefficient for the bimolecular reaction of propargyl radical with NO_2, $(2.55 \pm 0.05) \times 10^{-11}$ cm^3 $molecule^{-1}$ s^{-1}, is 40% lower than the values given above for the vinyl and allyl radicals. Thus, the resonance stabilization has only a small effect on the reactivity of unsaturated hydrocarbon radicals with NO_2. Finally, chlorine substitution reduces the reactivity of unsaturated hydrocarbon radicals with NO_2, as concluded from the obtained rate coefficient for the bimolecular reaction of the 1,2-dichloroallyl radical with NO_2 at 300 K, $(2.37 \pm 0.05) \times 10^{-11}$ cm^3 $molecule^{-1}$ s^{-1}, which is 40% lower than the value given above for the unsubstituted allyl radical.

Conclusions

Bimolecular rate coefficients of the $C_2H_3 + NO_2$ and $C_3H_3 + NO_2$ reactions have been measured in the temperature range 220−340 K and have been found to obey the following expressions: $k(C_2H_3 + NO_2) = [(4.19 \pm 0.05) \times 10^{-11}](T/300\ K)^{-0.60\pm0.07}$ cm^3 $molecule^{-1}$ s^{-1} and $k(C_3H_3 + NO_2) = [(2.55 \pm 0.05) \times 10^{-11}](T/300\ K)^{-1.06\pm0.10}$ cm^3 $molecule^{-1}$ s^{-1}, respectively. The bimolecular reaction rate coefficient of the 1,2-dichloroallyl radical with NO_2 at 298 K has also been determined: $k(C_3H_3Cl_2 + NO_2) = (2.37 \pm 0.05) \times 10^{-11}$ cm^3 $molecule^{-1}$ s^{-1}. The absence of bath gas pressure dependence of the reaction rates rules out the importance of three-body processes in these systems. For the $C_2H_3 + NO_2$ reaction, NO has been detected as a product. No experimental evidence of an activation barrier has been observed for the $C_2H_3 + NO_2$ and $C_3H_3 + NO_2$ reactions.

Ab initio calculations are used to explain the experimental findings. An attack of the vinyl radical on the N-atom site of NO_2 is suggested to be dominant in the $C_2H_3 + NO_2$ reaction. Nitroethylene formed can undergo isomerization to vinyl nitrite and subsequently eliminate NO and form vinyloxy radical. In the $C_3H_3 + NO_2$ reaction, a barrierless attack on the O atom of NO_2 is found to be possible, leading to either allenyl nitrite or propargyl nitrite. Both intermediates can undergo a breaking of the N−O bond to form NO as well as allenyloxy and propargyloxy radicals, respectively. The ab initio results are in good agreement with the experimental findings, supporting the use of high-level electronic structure calculations to obtain insight in understanding experimental observations in gas kinetics.

Acknowledgment. W.D.G. acknowledges support from a TMR fellowship under the "Improving Human Potential and the Socio-economic Knowledge Database" program of the European Union (contract no. HPRN-CT-2000-00022). A.J.E. thanks the KONE foundation for research grant. R.S.T. also acknowledges support from the Bioscience and Environmental Research Council of Academy of Finland and Maj and Tor Nessling Foundation. L.H. thanks the Natural Science and Engineering Research Council of Academy of Finland for financial support. The authors are also indebted to the CSC Ltd in Espoo, Finland, for computer time.

Supporting Information Available: Results of the quantum chemical calculations: energies of the reactants, intermediates and products of the $C_2H_3 + NO_2$ and $C_3H_3 + NO_2$ reactions

(Table 1S); vibrational frequencies of the intermediates of the $C_2H_3 + NO_2$ and $C_3H_3 + NO_2$ reactions (Table 2S); structures of the intermediates of the $C_2H_3 + NO_2$ and $C_3H_3 + NO_2$ reactions (Table 3S). This material is available free of charge via the Internet at http://pubs.acs.org.

References and Notes

(1) Richter, H.; Howard, J. B. *Prog. Energy Combust. Sci.* **2000**, *26*, 565.

(2) Frenklach, M. *Phys. Chem. Chem. Phys.* **2002**, *4*, 2028.

(3) Goos, E.; Hippler, H.; Hoyermann, K.; Jürges, B. *Phys. Chem. Chem. Phys.* **2002**, *4*, 2011.

(4) Knyazev, V. D.; Slagle, I. R. *J. Phys. Chem.* **1995**, *99*, 2247.

(5) Eskola, A. J.; Timonen, R. S. *Phys. Chem. Chem. Phys.* **2003**, *5*, 2557.

(6) Atkinson, D. B.; Hudgens, J. W. *J. Phys. Chem. A* **1999**, *103*, 4242.

(7) Hahn, D. K.; Klippenstein, S. J.; Miller, J. A. *Faraday Discuss.* **2001**, *119*, 79.

(8) Richter, H.; Howard, J. B. *Phys. Chem. Chem. Phys.* **2002**, *4*, 2038.

(9) Marinov, N. M.; Pitz, W. J.; Westbrook, C. K.; Vincitore, A. M.; Castaldi, M. J.; Senkan, S. M.; Melius, C. F. *Combust. Flame* **1998**, *114*, 192.

(10) *NIST Chemical Kinetics Database, Standard Reference Database 17-2Q98*; National Institute of Standards and Technology: Gaithersburg, MD 20899.

(11) Slagle, I. R.; Yamada, F.; Gutman, D. *J. Am. Chem. Soc*. **1981**, *103*, 149.

(12) Krokidis, X.; Moriarty, N. W.; Lester W. A., Jr.; Frenklach, M. *Chem. Phys. Lett.* **1999**, *314*, 534.

(13) Paraskevopoulos, G.; Cvetanović, R. J. *J. Phys. Chem.* **1977**, *81*, 2598.

(14) Slagle, I. R.; Gutman, D. *Proc. Combust. Inst.* **1986**, *21*, 875.

(15) Fahr, A.; Braun, W.; Laufer, A. H. *J. Phys. Chem.* **1993**, *97*, 1502.

(16) Slagle, I. R.; Park, J.-Y.; Heaven, M. C.; Gutman, D. *J. Am. Chem. Soc.* **1984**, *106*, 4356.

(17) Morter, C. L.; Farhat, S. K.; Adamson, J. D.; Glass, G. P.; Curl, R. F. *J. Phys. Chem.* **1994**, *98*, 7029.

(18) Atkinson, D. B.; Hudgens, J. W. *J. Phys. Chem. A* **1999**, *103*, 7978.

(19) Hudgens, J. W.; Gonzalez, C. *J. Phys. Chem. A* **2002**, *106*, 6143.

(20) Lias, S. G. Ionization Energy Evaluation. In *NIST Chemistry WebBook, NIST Standard Reference Database Number 69*; Linstrom, P. J., Mallard, W. G., Eds.; National Institute of Standards and Technology: Gaithersburg, MD 20899, March 2003 (http://webbook.nist.gov).

(21) Frisch, M. J.; Trucks, G. W.; Schlegel, H. B.; Scuseria, G. E.; Robb, M. A.; Cheeseman, J. R.; Zakrzewski, V. G.; Montgomery, J. A., Jr.; Stratmann, R. E.; Burant, J. C.; Dapprich, S.; Millam, J. M.; Daniels, A. D.; Kudin, K. N.; Strain, M. C.; Farkas, O.; Tomasi, J.; Barone, V.; Cossi, M.; Cammi, R.; Mennucci, B.; Pomelli, C.; Adamo, C.; Clifford, S.; Ochterski, J.; Petersson, G. A.; Ayala, P. Y.; Cui, Q.; Morokuma, K.; Rega, N.; Salvador, P.; Dannenberg, J. J.; Malick, D. K.; Rabuck, A. D.; Raghavachari, K.; Foresman, J. B.; Cioslowski, J.; Ortiz, J. V.; Baboul, A. G.; Stefanov, B. B.; Liu, G.; Liashenko, A.; Piskorz, P.; Komaromi, I.; Gomperts, R.; Martin, R. L.; Fox, D. J.; Keith, T.; Al-Laham, M. A.; Peng, C. Y.; Nanayakkara, A.; Challacombe, M.; Gill, P. M. W.; Johnson, B.; Chen, W.; Wong, M. W.; Andres, J. L.; Gonzalez, C.; Head-Gordon, M.; Replogle, E. S.; Pople, J. A. *Gaussian 98*, Revision A.11.4; Gaussian, Inc.: Pittsburgh, PA, 2002.

(22) Barnhard, K. I.; Santiago, A.; He M.; Asmar, F.; Weiner, B. R. *Chem. Phys. Lett.* **1991**, *178*, 150.

(23) Sun, F.; Glass, G. P.; Curl, R. F. *Chem. Phys. Lett.* **2001**, *337*, 72.

(24) Harwood, M. H.; Jones, R. L. *J. Geophys. Res.* **1994**, *99*, 22955.

(25) Borrel, P.; Cobos, C. J.; Luther, K. *J. Phys. Chem.* **1988**, *92*, 4377.

(26) Kaufman, F. *Progress in Reaction Kinetics*; Porter, G., Ed.; Pergamon: New York, 1961; Vol. 1, p 1.

(27) Timonen, R. S.; Seetula, J. A.; Gutman, D. *J. Phys. Chem.* **1993**, *97*, 8217.

(28) Wickham, A. G.; Clary, D. C. *J. Chem. Phys.* **1993**, *98*, 420.

(29) Sims, I. R.; Queffelec, J.-L.; Defrance, A.; Rebrion-Rowe C.; Travers, D.; Bocherel, P.; Rowe, B. R.; Smith, I. W. M. *J. Chem. Phys.* **1994**, *100*, 4229.

(30) Maergoiz, A. I.; Nikitin, E. E.; Troe, J. *J. Chem. Phys.* **1995**, *103*, 2083.

(31) Sims, I. R.; Smith, I. W. M. *Annu. Rev. Phys. Chem.* **1995**, *46*, 109.

(32) DeSain, J. D.; Hung, P. Y.; Thompson, R. I.; Glass, G. P.; Scuseria, G.; Curl, R. F. *J. Phys. Chem. A* **2000**, *104*, 3356.

(33) Cooksy, A. L. *J. Phys. Chem. A* **1998**, *102*, 5093.

(34) Gindulyte, A.; Massa, L.; Huang, L.; Karle, J. *J. Phys. Chem. A* **1999**, *103*, 11045.

(35) Seminario, J. M.; Politizer, P. *Int. J. Quantum Chem., Quantum Chem. Symp.* **1992**, *26*, 497.

(36) Packwood, T. J.; Page, M. *Chem. Phys. Lett.* **1993**, *216*, 180.

(37) Wodtke, A. M.; Hintsa, E. J.; Lee, Y. T. *J. Phys. Chem.* **1986**, *90*, 3549.

(38) Gindulyté, A.; Massa, L.; Huang, L.; Karle, J. *J. Phys. Chem. A* **1999**, *103*, 11040.

(39) McAllister, M. A.; Tidwell, T. T. *J. Org. Chem*. **1994**, *59*, 4506.

(40) Rall, K. B.; Vil'davskaya, A. I.; Petrov, A. A. *Zh. Org. Khim.* **1982**, *18*, 2469.